Human Molecular Genetics, 2010, Vol. 19, No. 7 ***1199–1210***
doi:10.1093/hmg/ddp590
Advance Access published on January 6, 2010

Gain-of-function mutation in FGFR3 in mice leads to decreased bone mass by affecting both osteoblastogenesis and osteoclastogenesis

Nan Su[1,†], Qidi Sun[1,†], Can Li[1], Xiumin Lu[1], Huabing Qi[1], Siyu Chen[1], Jing Yang[1], Xiaolan Du[1], Ling Zhao[1], Qifen He[1], Min Jin[1], Yue Shen[1], Di Chen[2] and Lin Chen[1,*]

[1]State Key Laboratory of Trauma, Burns and Combined Injury, Trauma Center, Institute of Surgery Research, Daping Hospital, Third Military Medical University, Chongqing 400042, China and [2]Department of Orthopaedics, University of Rochester, Rochester, NY 14642, USA

Received September 13, 2009; Revised November 26, 2009; Accepted December 31, 2009

Achondroplasia (ACH) is a short-limbed dwarfism resulting from gain-of-function mutations in fibroblast growth factor receptor 3 (FGFR3). Previous studies have shown that ACH patients have impaired chondrogenesis, but the effects of FGFR3 on bone formation and bone remodeling at adult stages of ACH have not been fully investigated. Using micro-computed tomography and histomorphometric analyses, we found that 2-month-old *Fgfr3*$^{G369C/+}$ mice (mouse model mimicking human ACH) showed decreased bone mass due to reduced trabecular bone volume and bone mineral density, defect in bone mineralization and increased osteoclast numbers and activity. Compared with primary cultures of bone marrow stromal cells (BMSCs) from wild-type mice, *Fgfr3*$^{G369C/+}$ cultures showed decreased cell proliferation, increased osteogenic differentiation including up-regulation of alkaline phosphatase activity and expressions of osteoblast marker genes, and reduced bone matrix mineralization. Furthermore, our studies also suggest that decreased cell proliferation and enhanced osteogenic differentiation observed in *Fgfr3*$^{G369C/+}$ BMSCs are caused by up-regulation of p38 phosphorylation and that enhanced Erk1/2 activity is responsible for the impaired bone matrix mineralization. In addition, *in vitro* osteoclast formation and bone resorption assays demonstrated that osteoclast numbers and bone resorption area were increased in cultured bone marrow cells derived from *Fgfr3*$^{G369C/+}$ mice. These findings demonstrate that gain-of-function mutation in FGFR3 leads to decreased bone mass by regulating both osteoblast and osteoclast activities. Our studies provide new insight into the mechanism underlying the development of ACH.

INTRODUCTION

Fibroblast growth factor receptor 3 (FGFR3) is one of a family of four membrane-bound receptor tyrosine kinases (FGFR1–4) that mediates signals from many of the 22 fibroblast growth factors (FGF1–22). FGFR3 is a negative regulator of endochondral bone development (1,2). Gain-of-function mutations in FGFR3 result in chondrodysplasias which include achondroplasia (ACH), hypochondroplasia and thanatophoric dysplasia (TD) (2–4). In contrast, partial loss-of-function mutation of FGFR3 causes camptodactyly, tall stature, scoliosis and hearing loss (CATSHL) syndrome (5).

ACH is characterized by the short limb dwarfism, spinal stenosis and facial dysmorphism, which is the most common hereditary dwarfism with an incidence rate between 1/15 000 and 1/40 000 live births (6). Although gain-of-function mutations of FGFR3 in ACH have been found to inhibit the proliferation and differentiation of chondrocytes and subsequently cause shortened long bone resulting in dwarfism (7–11), the effects of FGFR3 on the postnatal bone formation and bone remodeling in ACH have not been well elucidated.

During postnatal and adult stages, bone undergoes continuous remodeling through the coordinated processes of bone

*To whom correspondence should be addressed. Tel: +86 2368702991; Fax: +86 2368702991; Email: linchen70@163.com
†These authors contributed equally to this work.

formation and bone resorption (12,13). Evidence suggests that FGFR3 is involved in bone formation. FGFR3 can affect intramembranous ossification. Two gain-of-function mutations of FGFR3 (P250R and A391E) have been identified in humans resulting in Muenke syndrome, and Crouzon syndrome with Acanthosis Nigricans. Both syndromes have premature fusion of the cranial sutures (2,14–17). Furthermore, TD is also frequently associated with severe craniosynostosis (18), although Karadimas reported that a patient with ACH resulting from G380R mutation in FGFR3 had multiple-suture synostosis (19). Additionally, adult *Fgfr3* and *Fgfr3IIIc* null mutant mice showed osteopenia and defects in bone matrix mineralization (20,21). These studies indicate that FGFR3 could regulate bone formation and remodeling.

Our previous study showed shortened trabecular bone and increased expressions of osteoblast markers such as core binding factor a1 (*Cbfa1*), osteopontin (*OP*) and osteocalcin (*OC*) in the growth plate of $Fgfr3^{G369C/+}$ mice (a mouse model mimicking human ACH resulting from the gain-of-function mutation, Gly375Cys, of FGFR3) on postnatal day 15 (11). These data indicate that activation of FGFR3 could influence bone formation at an early age of ACH, but the characteristics of the bone formation and bone remodeling in adult ACH mice are not clear.

In postnatal and adult skeleton, bone mass is maintained through the close micro-anatomical coupling of osteoblastic and osteoclastic activities. However, the actual effect of the activated mutation of FGFR3 on osteoclastogenesis in adult ACH and its mechanism is not clear.

To determine the status of bone formation and remodeling in adult ACH and its underlying mechanisms, we have characterized adult $Fgfr3^{G369C/+}$ mice. Our results revealed that a gain-of-function mutation (G369C) in FGFR3 in mice led to decreased bone mass by inhibiting the proliferation and mineralization of bone marrow stromal cells (BMSCs) and promoting osteoclast formation and activity. Furthermore, we showed that the Erk1/2 and p38 pathways are involved in the regulation of proliferation, osteogenic differentiation and bone matrix mineralization of the cultured BMSCs with activated FGFR3.

RESULTS

Gain-of-function mutation of FGFR3 results in decreased bone mass

Radiological analysis of femurs from 2- to 4-month-old mice showed that $Fgfr3^{G369C/+}$ mice exhibited short and sparse trabeculae compared with wild-type mice (Fig. 1A and B, arrows). The bone mineral density (BMD) of mutant mice and their littermate controls was also assessed at 2 and 4 months of age. The results showed that the BMD of the whole femurs of mutant mice, compared with wild-type mice, was reduced by 11 and 14% at 2 and 4 months, respectively (Fig. 1C).

To determine the structural parameters of trabecular bone, we performed micro-computed tomography (micro-CT) analysis of the distal metaphysis of femurs harvested from 2-month-old mice. Three-dimensional images of the femoral metaphysis are shown in Figure 1D. Trabecular bone number was decreased in mutant mice, which was consistent with the result of X-ray analysis. Quantification of the structural parameters revealed that bone volume/tissue volume (%, BV/TV), trabecular number (Tb.N) and trabecular thickness (Tb.Th) were decreased by 61%, 41% ($P < 0.05$) and 24% ($P < 0.01$), respectively (Fig. 1E–G). Trabecular separation (Tb.Sp) in mutant mice was significantly increased by 36% ($P < 0.05$; Fig. 1H). The decreased trabecular connectivity of $Fgfr3^{G369C/+}$ femora was confirmed by a significant increase in structure model index (SMI; Fig. 1I). Collectively, these observations indicate that activated mutation in FGFR3 caused decreased bone mass and compromised architecture in adult mice.

Altered bone formation in $Fgfr3^{G369C/+}$ mice

To determine whether the reduced bone mass in $Fgfr3^{G369C/+}$ mice was due to decreased bone formation, we performed a histologic analysis of decalcified and undecalcified tibiae. Von Kossa staining of undecalcified tibiae from 2-month-old mice showed that the trabecular bone of $Fgfr3^{G369C/+}$ mice was shorter and sparser than that of wild-type mice (Fig. 2A and B). The histomorphometric parameters of bone formation in the right proximal tibiae are shown in Figure 2I–K. The BV/TV and Tb.Th in $Fgfr3^{G369C/+}$ tibiae were significantly reduced by 44 and 29% ($P < 0.01$), respectively (Fig. 2I and J). Tb.Sp was significantly increased by 50% in mutant mice ($P < 0.05$; Fig. 2K). These results are consistent with the results obtained by micro-CT examination. Although the bone mass was decreased in $Fgfr3^{G369C/+}$ mice, the osteoblasts lining trabecular bone of $Fgfr3^{G369C/+}$ mice were larger and more cuboidal than those in wild-type mice (Fig. 2C and D, arrows), which suggests that the osteoblast activity in $Fgfr3^{G369C/+}$ mice was enhanced.

In $Fgfr3^{G369C/+}$ mice, the trabecular bone was lined with thicker osteoid compared with wild-type mice (Fig. 2E and F, arrows). The dynamics of bone formation at the metaphysis of tibiae were quantitatively evaluated by double labeling of calcein. A significant decrease in calcein labeling of mineralizing surfaces and reduced mineral appositional rates (MAR) was found in $Fgfr3^{G369C/+}$ mice ($P < 0.05$; Fig. 2G, H and L). The increased thickness of osteoid and decreased MAR in $Fgfr3^{G369C/+}$ mice suggests that there may be defects in bone matrix mineralization in $Fgfr3^{G369C/+}$ mice. All these bone phenotypes indicate that $Fgfr3^{G369C/+}$ mice have osteomalacia-like skeleton, which need to be further studied.

$Fgfr3^{G369C/+}$ mice show no remarkable changes in serum levels of Ca and phosphate, but had increased serum content of PINP

To investigate whether bone defects observed in $Fgfr3^{G369C/+}$ mice are related to systemic alteration in mineral homeostasis, we measured levels of total Ca and phosphate in mouse serum. Figure 3A shows that no significant differences in serum levels of both total Ca and phosphate were found between the control and mutant mice. N-terminal propeptide of type I procollagen (PINP) is a sensitive and specific marker for osteoblast activity. We detected the serum level of PINP using ELISA and found that the serum level of PINP was increased in

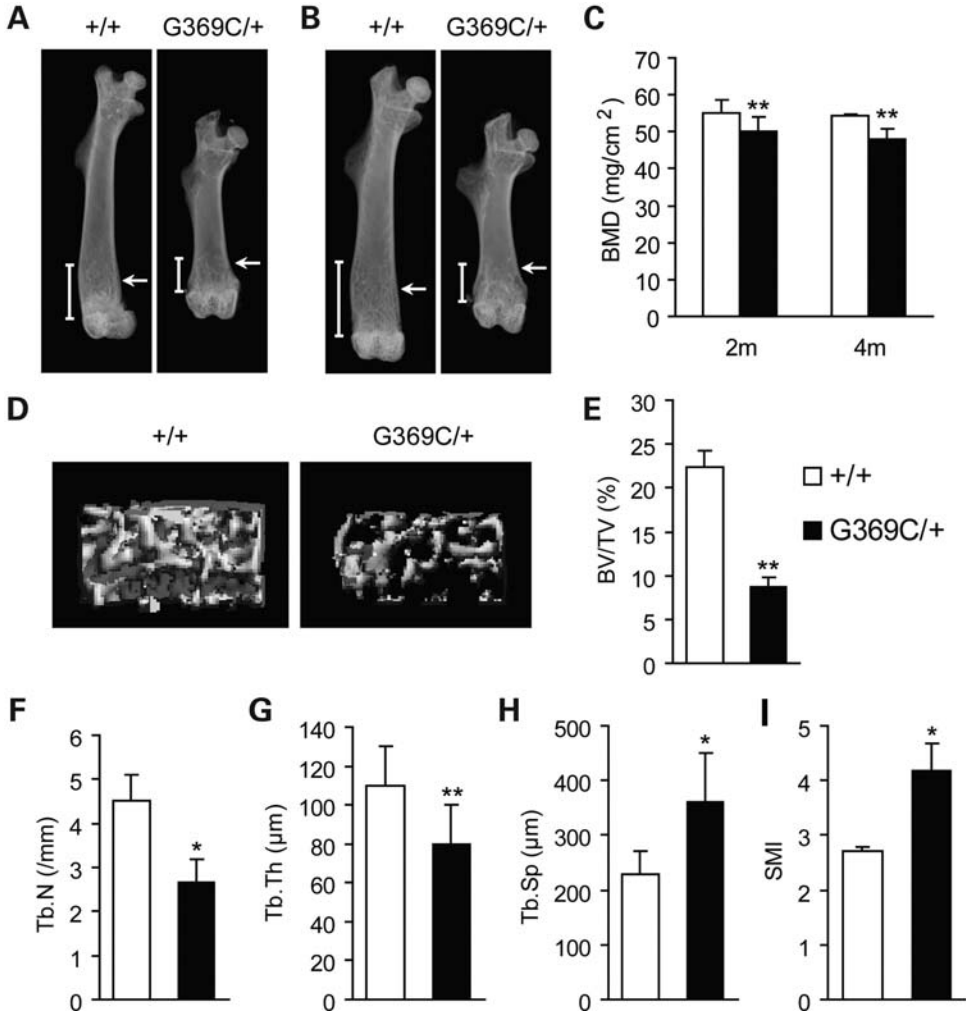

Figure 1. *Fgfr3*$^{G369C/+}$ mice had decreased bone mass compared with wild-type mice. (**A** and **B**) Faxitron X-ray analysis of total femurs from wild-type (+/+) and *Fgfr3*$^{G369C/+}$ mice (G369C/+) at 2 months (A) and 4 months (B) of age revealed short and sparse trabeculae in mutant mice (arrows). (**C**) BMD of femurs from *Fgfr3*$^{G369C/+}$ mice was significantly reduced compared with wild-type mice at 2 and 4 months ($n = 6$). (**D**–**I**) Quantitative micro-CT analyses of distal femoral metaphysis from wild-type and *Fgfr3*$^{G369C/+}$ mice at 2 months. Three-dimensional images showed reduced trabecular bone in mutant mice (D). Quantification of the structural parameters of the femoral metaphysis revealed that BV/TV, Tb.N and Tb.Th were significantly decreased, although Tb.Sp and SMI were significantly increased in mutant mice relative to wild-type mice ($n = 6$) (E–I). Graphs show mean value ± SD (Student's *t*-test, $^{*}P < 0.05$, $^{**}P < 0.01$).

Fgfr3$^{G369C/+}$mice (Fig. 3B), suggesting that osteoblast activity was increased in *Fgfr3*$^{G369C/+}$mice.

Gain-of-function mutation of FGFR3 affects the proliferation, osteogenic differentiation and bone matrix mineralization of BMSCs

To further explore the mechanism for the altered bone formation in *Fgfr*$^{G369C/+}$ mice, we cultured BMSCs to evaluate changes in cell proliferation and osteogenic differentiation. Using an *in vitro* colorimetric assay, we found that cell proliferation was decreased in BMSCs derived from *Fgfr*$^{G369C/+}$ mice compared with that of wild-type BMSCs (Fig. 4A). To determine changes in osteogenic differentiation of BMSCs, we compared the formation of alkaline phosphatase (ALP)-positive colonies, the ALP activity and numbers of mineralized bone nodules (Alizarin red staining) in BMSCs isolated from both wild-type and *Fgfr3*$^{G369C/+}$ mice. After 7, 14 and 21 days of culture, the BMSCs from *Fgfr3*$^{G369C/+}$ mice showed increased number of crystal violet-staining cells (Fig. 4B). The ALP activity of BMSCs was significantly increased in *Fgfr3*$^{G369C/+}$ mice (Fig. 4C). On day 14 and 21, *Fgfr3*$^{G369C/+}$ BMSCs had fewer mineralized colonies and decreased absorbance of alizarin red (Fig. 4D and E). These results suggest that gain-of-function mutation of FGFR3 inhibited the BMSC proliferation and promoted their osteogenic differentiation, but blocked their mineralization.

RNA harvested from BMSCs after 7 days of culture was used to measure the expressions of genes related to osteogenic differentiation using real-time PCR. As shown in Figure 4F, the expression levels of *Cbfa1*, *OP*, *OC* and type I collagen (*Col1a1*) of BMSCs were all increased in *Fgfr3*$^{G369C/+}$ mice compared with wild-type mice. These results further indicate that gain-of-function mutation of FGFR3 could promote osteogenic differentiation of BMSCs.

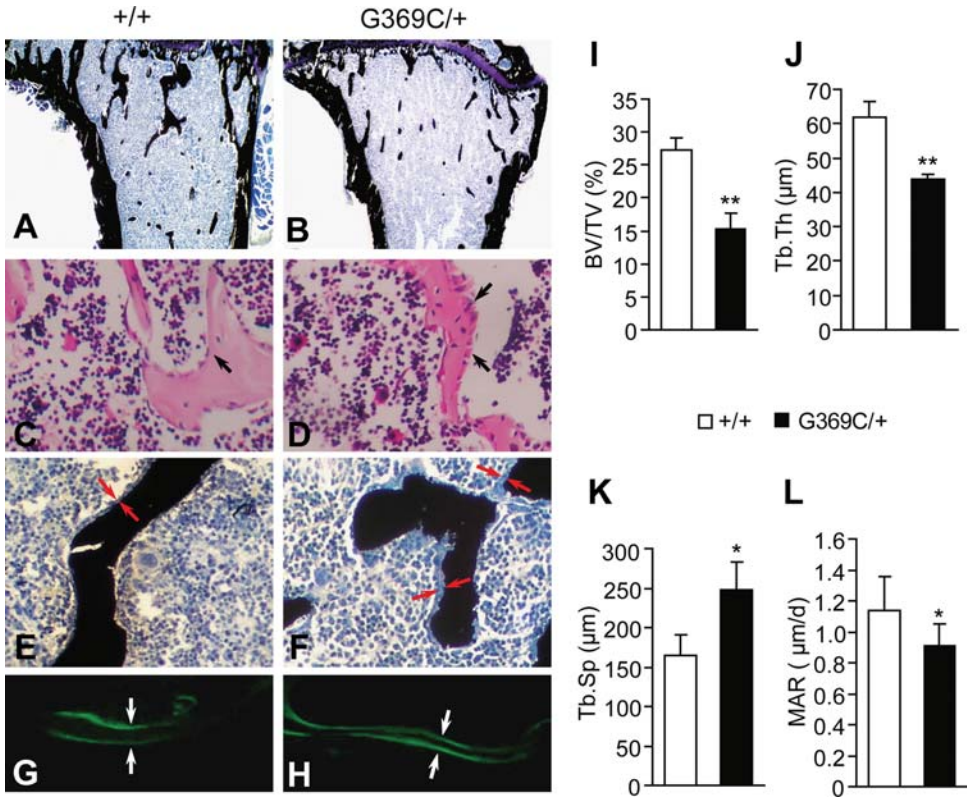

Figure 2. Histochemical analysis of decalcified and undecalcified tibiae from 2-month-old wild-type (+/+) and *Fgfr3*$^{G369C/+}$ mice (G369C/+). (**A** and **B**) Von Kossa staining of undecalcified tibiae revealed that the proximal tibiae of 2-month-old *Fgfr3*$^{G369C/+}$ mice had shorter and sparser trabecular bone compared with wild-type mice (magnification, ×40). (**C** and **D**) H&E staining of tibiae showed the morphology of metaphyseal osteoblasts in the proximal tibia. Note that osteoblasts lining trabecular bone in the *Fgfr3*$^{G369C/+}$ mice were more plump and cuboidal (arrows; magnification, ×400). (**E** and **F**) Von Kossa staining showed that osteoid laid down in the trabecular bone in *Fgfr3*$^{G369C/+}$ mice was thicker compared with wild-type mice (red arrows; magnification, ×400). (**G** and **H**) Double calcein labeling of undecalcified tibiae. White arrows specify distance between labeled bone surfaces. Labeling for calcein was significantly reduced in the *Fgfr3*$^{G369C/+}$ mice (H) compared with wild-type controls (G) (magnification, ×400). (**I**–**L**) Histomorphometric measurements of tibiae. The tibiae from *Fgfr3*$^{G369C/+}$ mice had decreased BV/TV, Tb.Th and MAR, but significantly increased Tb.Sp ($n = 5$). Graphs show mean value ± SD (Student's *t*-test, $^{*}P < 0.05$, $^{**}P < 0.01$).

FGFR3 regulates the proliferation, osteogenic differentiation and matrix mineralization of BMSCs through Erk1/2 and p38 MAPK pathways

FGFs/FGFRs can exert their effects through the MAPK pathways, including the extracellular signal-related kinase1/2 (Erk1/2) and p38 MAPK (2), which play important roles in bone formation (22,23). We detected the expression levels of phosphorylated Erk1/2 and p38 of wild-type and *Fgfr3*$^{G369C/+}$ BMSCs. The result showed increased phosphorylation level of Erk1/2 and p38 in *Fgfr3*$^{G369C/+}$ BMSCs (Fig. 5A), which indicates that Erk1/2 and p38 signaling may participate in the regulation of bone formation by FGFR3.

To determine if Erk1/2 and p38 were indeed involved in the bone phenotypes of *Fgfr3*$^{G369C/+}$ mice, we investigated the effects of Erk1/2 and p38 on the proliferation, ALP activity and matrix mineralization in cultured BMSCs by using specific inhibitor against either Erk1/2 or p38. The *in vitro* colorimetric assay for cell growth showed that cell proliferation of *Fgfr3*$^{G369C/+}$ BMSCs was further inhibited by the treatment with Erk1/2 inhibitor (PD98059). In contrast, cell proliferation was increased following the treatment with SB203580, an inhibitor of p38, after 5 days of culture (Fig. 5C). Figure 5D and E showed that the originally increased ALP activity of *Fgfr3*$^{G369C/+}$ BMSCs was further increased after *Fgfr3*$^{G369C/+}$ BMSCs were treated with PD98059 for 7 days in osteoblast differentiation medium. However, ALP activity was inhibited by SB203580 in both wild-type and *Fgfr3*$^{G369C/+}$ BMSCs. After 14 days, the mineralized nodules and mineral content in both *Fgfr3*$^{G369C/+}$ and wild-type BMSCs were significantly increased after treatment with PD98059, but they were significantly reduced after SB203580 treatment (Fig. 5F and G). Furthermore, analyses of osteoblast marker genes showed that the levels of *Cbfa1* and *OC* mRNA were significantly up-regulated by the treatment with PD98059 (7 days) in both wild-type and *Fgfr3*$^{G369C/+}$ BMSCs, but were decreased following SB203580 treatment (Fig. 5H and I). All these results suggest that Erk1/2 and p38 have distinct role in osteoblastogenesis. Erk1/2 promotes proliferation, but inhibits the osteogenic differentiation and mineralization, although p38 inhibits the proliferation, but promotes differentiation and mineralization of BMSCs.

Gain-of-function mutation of FGFR3 promotes osteoclast formation and bone resorption

Bone remodeling is a process that includes the tight coupling between bone formation and bone resorption. Since the

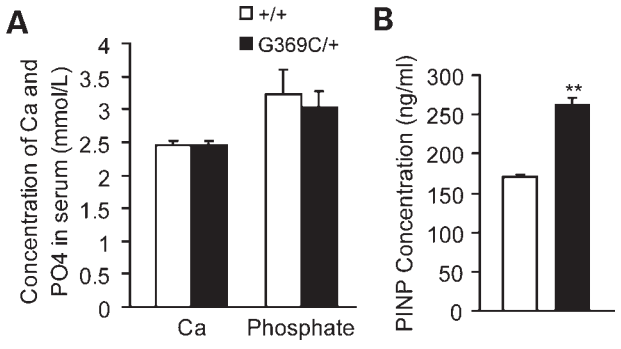

Figure 3. Serum biochemistry and serum level of PINP of 2-month-old wild-type and *Fgfr3*$^{G369C/+}$ mice. (**A**) There was no remarkable difference of serum level of total Ca and phosphate between wild-type and mutant mice ($n = 6$). (**B**) The serum level of PINP measured by ELISA was significantly increased in mutant mice compared with wild-type mice ($n = 6$). Graphs show mean value $\pm$ SD (Student's *t*-test, $^{**}P < 0.01$).

Fgfr3$^{G369C/+}$ mice showed decreased bone mass, we examined if these changes are also related to the alterations in osteoclast activity. Figure 6A and B show that the number of tartrate-resistant acid phosphatase (TRAP)-positive osteoclasts in *Fgfr3*$^{G369C/+}$ mice was increased compared with wild-type mice. Furthermore, the areas of resorption pits were also larger in *Fgfr3*$^{G369C/+}$ mice. These results suggest that the activated mutation of FGFR3 stimulated osteoclastogenesis.

To determine if FGFR3 had effect on osteoclast differentiation, *in vitro* osteoclast formation assay was performed using cultures of bone marrow osteoclast precursors treated with M-CSF and RANKL. We first identified the expression of FGFR3 in osteoclasts (data not shown), indicating that FGFR3 might directly regulate the differentiation and function of osteoclasts. After 10 days in culture, TRAP staining showed that the number of TRAP-positive cells with large multinucleus was significantly increased in cultures derived from *Fgfr3*$^{G369C/+}$ mice compared with those from wild-type mice (Fig. 6C and D), indicating that FGFR3 can directly promote osteoclast differentiation. Furthermore, we used bone resorption assay to detect whether gain-of-function mutation of FGFR3 could affect the resorption activity of osteoclasts. Our result showed that the bone resorption area of *Fgfr3*$^{G369C/+}$ osteoclasts on day 15 was larger than that of wild-type osteoclasts (Fig. 6E and F), suggesting that the resorption activity of *Fgfr3*$^{G369C/+}$ osteoclasts was enhanced. We also examined the expression of genes related to osteoclastogenesis. Real-time PCR analysis of mRNA from osteoclasts cultured in differentiation medium for 10 days showed that the mRNA levels of *TRAP* and *MMP-9* were up-regulated in osteoclasts derived from *Fgfr3*$^{G369C/+}$ mice, but there was no significant difference between the expression level of *Cathepsin K* (*Ctsk*) in mice of both genotypes (Fig. 6G). These results further confirm that gain-of-function mutation of FGFR3 promoted the osteoclast formation and bone resorption activity directly.

DISCUSSION

ACH is the most common form of dwarfisms in humans, the phenotype of which is thought to be caused mainly by severely disturbed chondrogenesis resulting from gain-of-function mutations in FGFR3 (1,9). However, the status of bone formation and bone remodeling in adult ACH is not well characterized. The maintenance of bone mass in adult depends on the balance between osteoblastogenesis and osteoclastogenesis. In this study, we used adult *Fgfr3*$^{G369C/+}$ mice to study the effect of the activated FGFR3 on bone mass and structure and its mechanism in ACH. The BV and BMD were decreased in the femurs of 2- and 4-month-old *Fgfr3*$^{G369C/+}$ mice. Structural analysis of bone by micro-CT and histomorphometry also demonstrated a marked reduction in bone mass in metaphysis of the femurs and tibiae from *Fgfr3*$^{G369C/+}$ mice. We further found that the decreased bone mass was caused by both altered bone formation and bone resorption.

FGFR3 promotes osteogenic differentiation of BMSCs but inhibits their mineralization

Osteoblasts, the cells responsible for bone formation, are differentiated from mesenchymal progenitor cells. Osteoblast differentiation is regulated by systemic and local factors, including FGFs/FGFRs (1,2,20,24,25). In *Fgfr3*$^{G369C/+}$ mice, bone formation is influenced by the activated FGFR3 signaling. Histologic and histomorphometric analyses showed that the number and thickness of trabecular bone were decreased in *Fgfr3*$^{G369C/+}$ mice. Although the bone mass of trabecular bone was reduced, osteoblasts lining trabecular bone in mutant mice were more plump and cuboidal than those in wild-type mice, indicating that the activity of osteoblasts in these mice was actually enhanced. On the other hand, the increased thickness of osteoid laid down in trabecular bone and decreased MAR in *Fgfr3*$^{G369C/+}$ mice indicate impaired mineralization. The comparable serum levels of Ca and phosphate between mutant and wild-type mice indicate that the altered osteoblast function was not likely related to the perturbation in mineral homeostasis, but was most likely caused by changes in the osteoblasts themselves. The cell culture studies further support our *in vivo* results. Cultured BMSCs from *Fgfr3*$^{G369C/+}$ mice showed enhanced ALP activity and impaired bone matrix mineralization.

Cbfa1 is an essential and indispensable transcription factor for osteoblasts differentiation from mesenchymal progenitor or precursors cells (26,27). *Cbfa1* positively regulates the expressions of several osteoblast-specific genes such as *OP* and *OC* (22,28). The expressions of *Cbfa1*, *OP* and *OC* were increased in *Fgfr3*$^{G369C/+}$ BMSCs on day 7, suggesting that gain-of-function mutation of FGFR3 promoted osteogenic differentiation via its up-regulation of *Cbfa1*. This result is consistent with other results reported. Chen *et al*. found that the expressions of *Cbfa1*, *OP* and *OC* were up-regulated in the growth plate of *Fgfr3*$^{G369C/+}$ mice on P15. Funato *et al.* (29) also discovered that FGFR3 stimulates osteoblast MG63 cell differentiation.

FGFR1 is another member of the FGF receptor family. Valverde-Franco *et al*. (20) found that the mRNA level of FGFR1 was increased in BMSCs of *Fgfr3* null mutant mice, and they proposed that FGFR1 is involved in the pathogenesis underlying the bone changes found in *Fgfr3* null mutant mice. To observe if FGFR1 also play a role in the bone phenotypes of ACH mice, we measured and found FGFR1 was unexpectedly

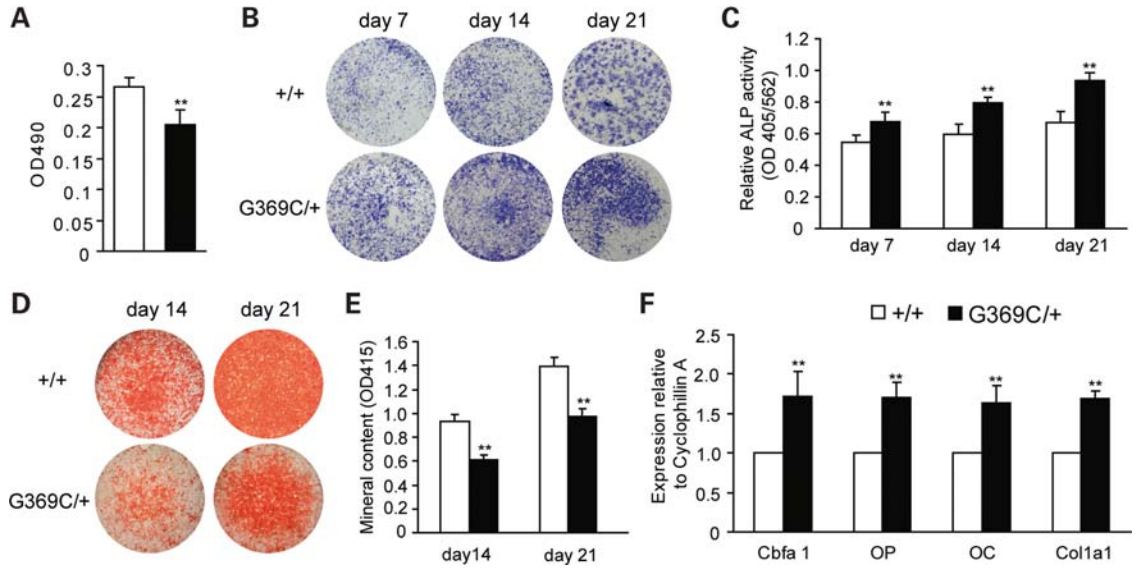

Figure 4. Effects of activated FGFR3 on the proliferation, osteogenic differentiation and mineralization of BMSCs. (**A**) MTT proliferation assay showed decreased proliferation of *Fgfr3*$^{G369C/+}$ BMSCs. (**B**) ALP staining showed increased crystal violet-staining cells in cultured *Fgfr3*$^{G369C/+}$ BMSCs compared with wild-type BMSCs on day 7, 14 and 21. (**C**) ALP activity (normalized to the total protein content of the sample, 562 nm) was significantly enhanced in *Fgfr3*$^{G369C/+}$ BMSCs. (**D**) Alizarin red staining of the mineralized osteoblasts showed decreased number of mineralized nodules on day 14 and 21 after osteogenic differentiation in *Fgfr3*$^{G369C/+}$ mice. (**E**) Bound alizarin red was dissolved with 0.5 N HCl, 5% SDS and measured at 415 nm to quantify the mineral content. Cultured *Fgfr3*$^{G369C/+}$ BMSCs showed reduced mineral content. (**F**) Relative expressions of osteogenic marker genes measured by qRT–PCR. The expression levels of *Cbfa1*, *OP*, *OC* and *Col1a1* mRNA in differentiated BMSCs were remarkably increased in *Fgfr3*$^{G369C/+}$ BMSCs on day 7. Graphs show mean value ± SD (Student's *t*-test, $^{**}P < 0.01$).

increased significantly in *Fgfr3*$^{G369C/+}$ BMSCs (our unpublished data). FGFR1 signaling has been found to regulate *Cbfa1* expression in osteoblasts and promote early osteoblastic differentiation (24,30), which can to some extent partially explain some phenotypes of *Fgfr3*$^{G369C/+}$ mice mentioned above. However, the gain-of-function mutation of FGFR1 in humans and mice causes craniosynostosis (Pfeiffer syndrome) and increased mineralization (30), which are not found in *Fgfr3*$^{G369C/+}$ mice. So we think that the bone phenotypes of *Fgfr3*$^{G369C/+}$ mice are more likely directly related to the activation of FGFR3, although we can not completely exclude the potential involvement of FGFR1 in it.

Erk1/2 and p38 MAPK pathways are differentially involved in the FGFR3-regulated BMSC proliferation, osteogenic differentiation and mineralization

The major downstream signaling pathways of FGFs/FGFRs are composed of the MAPK pathway (including the Erk1/2, p38 and JNK), the PI3-kinase and the PLC-γ pathway (1,2). MAPK is known for its role in bone formation and in mediating the effect of FGFs/FGFRs on osteoblast proliferation and differentiation (23,31,32). In *Fgfr3*$^{G369C/+}$ BMSCs, the levels of both phosphorylated Erk1/2 and p38 were increased, indicating that Erk1/2 and p38 signaling may be involved in the enhanced osteogenic differentiation, as well as the impaired proliferation and mineralization of BMSCs in *Fgfr3*$^{G369C/+}$ mice.

Previous studies have shown that Erk1/2 stimulates osteoblast proliferation (33–35), but negatively regulate the matrix mineralization (36). In our study, when Erk1/2 signaling pathway was inhibited by PD98059 in *Fgfr3*$^{G369C/+}$ BMSCs, the reduced cell proliferation was not reversed, but the decreased matrix mineralization was restored. These results suggest that Erk1/2 was not responsible for reduced cell proliferation, but for the impaired ability to mineralize observed in *Fgfr3*$^{G369C/+}$ BMSCs.

On the other hand, the increased osteogenic differentiation of *Fgfr3*$^{G369C/+}$ BMSCs was further enhanced after the inhibition of Erk1/2 pathway, which indicates that Erk1/2 signaling may negatively regulate osteogenic differentiation of BMSCs. Several studies support our findings. Continuous inhibition of MEK1 signaling promots the early osteoblastic differentiation in C2Cl2 pluripotent mesenchymal cells (37). BMSCs derived from osteoporotic patients also showed increased level of Erk1/2 phosphorylation compared with BMSCs derived from control donors (38). However, other studies also show that Erk1/2 signaling can positively regulate differentiation of primary osteoblast or MC3TC-E1 cells (23,32,39,40). These discrepancies may be related to different cells or cell lines used in these studies.

Our data also reveal that, besides Erk1/2, p38 MAPK signaling may be involved in the effect of FGFR3-regulated osteoblast proliferation and differentiation. In this study, when p38 MAPK was blocked with its specific inhibitor, the originally reduced proliferation of BMSCs in *Fgfr3*$^{G369C/+}$ mice was recovered. So we propose that p38 signaling is responsible for the inhibited proliferation of *Fgfr3*$^{G369C/+}$ BMSCs. Previous studies suggest that activation of p38 was involved in the FGF-induced growth arrest of chondrocytes (41), but the effect of p38 pathway activated by FGFR3 on the proliferation of BMSCs is not clear.

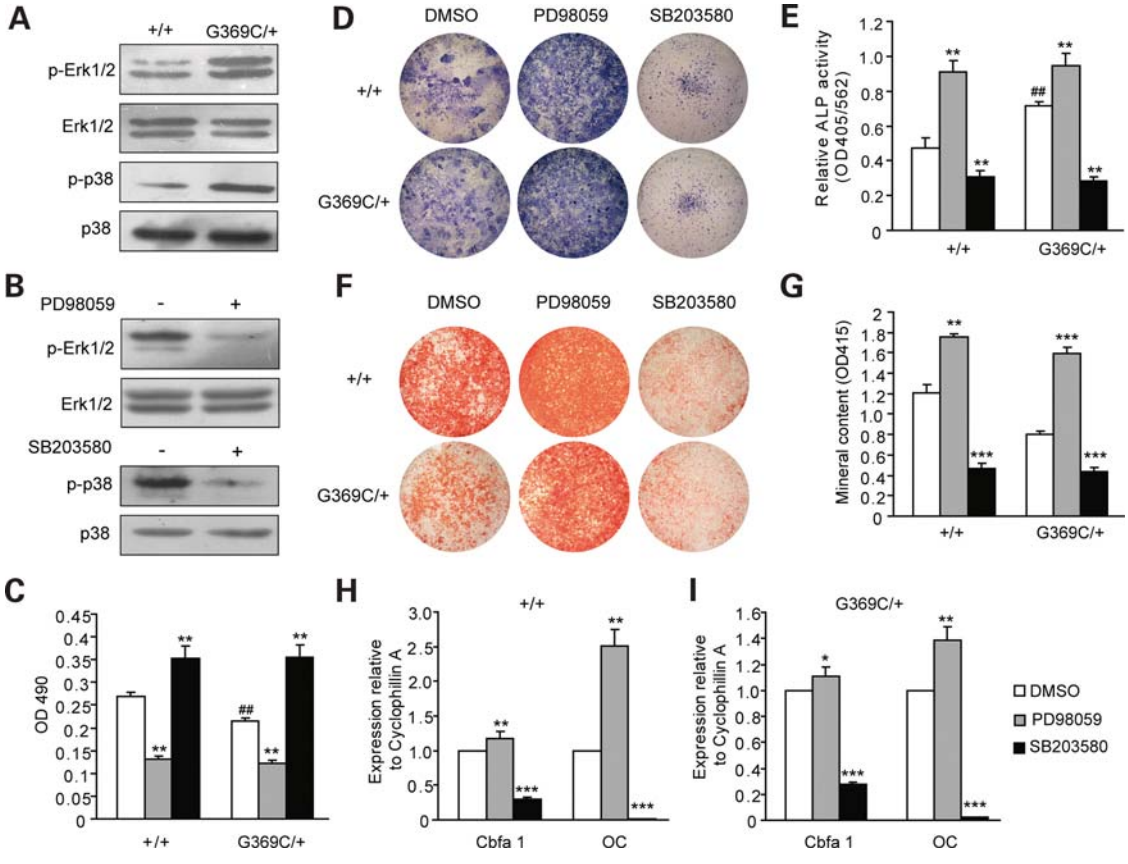

Figure 5. Erk1/2 and p38 MAPK pathway participated in the regulation of BMSCs by FGFR3. (**A**) Western blot analysis demonstrated that the levels of phospho-Erk1/2 and phospho-p38 were increased in *Fgfr3*$^{G369C/+}$ BMSCs cultured in basic medium. (**B**) Erk1/2 and p38 MAPK pathways were inhibited by PD98059 and SB203580, respectively. (**C**) The proliferation of both wild-type and *Fgfr3*$^{G369C/+}$ BMSCs was decreased in basic medium containing PD98059, but was increased in medium containing SB203580 after 5 days. (**D** and **E**) ALP staining and ALP activity analyses of BMSCs treated with PD98059 or SB203580 for 7 days. The ALP activity was increased in *Fgfr3*$^{G369C/+}$ BMSCs compared with wild-type BMSCs (##), and it was further enhanced in *Fgfr3*$^{G369C/+}$ BMSCs cultured in osteogenic differentiation medium containing PD98059 (**). However, both wild-type and *Fgfr3*$^{G369C/+}$ BMSCs treated with SB203580 showed decreased ALP activity compared with untreated BMSCs (**). (**F** and **G**) Alizarin red staining and quantification of mineral content of mineralized osteoblasts treated with PD98059 or SB203580 for 14 days. The mineralized nodules and mineral content of both *Fgfr3*$^{G369C/+}$ and wild-type BMSCs cultured in differentiation medium containing PD98059 were increased. However, they were significantly reduced after SB203580 treatment. (**H** and **I**) Relative expressions of osteogenic genes of BMSCs treated with PD98059 or SB203580 for 7 days. The expression levels of *Cbfa1* and *OC* were significantly increased in both wild-type (H) and *Fgfr3*$^{G369C/+}$ (I) BMSCs treated with PD98059, however, they were decreased after SB203580 treatment. Graphs show mean value ± SD (Student's *t*-test, $^{*}P < 0.05$, $^{**}P < 0.01$ and $^{***}P < 0.001$ versus untreated BMSCs, $^{\#\#}P < 0.01$ versus wild-type BMSCs).

Our study demonstrates for the first time that activation of FGFR3 leads to the growth arrest of BMSCs via p38 MAPK signaling.

P38 has also been found to stimulate osteogenesis *in vitro* by inducing *Cbfa1* expression, ALP activity and mineral deposition of BMSCs and osteoprogenitor cells (42–44). Our studies also showed that the increased osteogenic differentiation in *Fgfr3*$^{G369C/+}$ BMSCs was down-regulated after p38 signaling was inhibited, which suggests that p38 positively regulates the osteogenic differentiation of BMSCs. Since both Erk1/2 and p38 pathways are activated in *Fgfr3*$^{G369C/+}$ BMSCs, the increased osteogenic differentiation of the primarily cultured *Fgfr3*$^{G369C/+}$ BMSCs is more likely caused by the stimulatory effects of the activated p38 signaling on the osteogenic differentiation that overrides the inhibitory effect of Erk1/2. As for the mineralization, the already reduced matrix mineralization of *Fgfr3*$^{G369C/+}$ BMSCs was further impaired after inhibition of p38 signaling. We thus speculate that p38 signaling may be not responsible for the decreased mineralization resulting from gain-of-function mutation of FGFR3.

These data show that individual MAPK pathways have distinct roles in modulating the osteogenic development of *Fgfr3*$^{G369C/+}$ BMSCs (Fig. 7), and the phenotypes of *Fgfr3*$^{G369C/+}$ BMSCs include decreased proliferation, enhanced osteogenic differentiation and impaired mineralization, which were caused by the combination effect of the up-regulated Erk1/2 and p38 activity.

FGFR3 enhances osteoclastogenesis and bone resorption

The coupling between bone formation and bone resorption is essential for bone homeostasis (45). Osteoclasts are derived from the monocyte/macrophage hematopoietic precursor cells and are unique cells responsible for bone resorption (46,47). Two major mechanisms are involved in the regulation of osteoclast differentiation and bone resorption activity. One is the indirect regulation of osteoclast formation and function

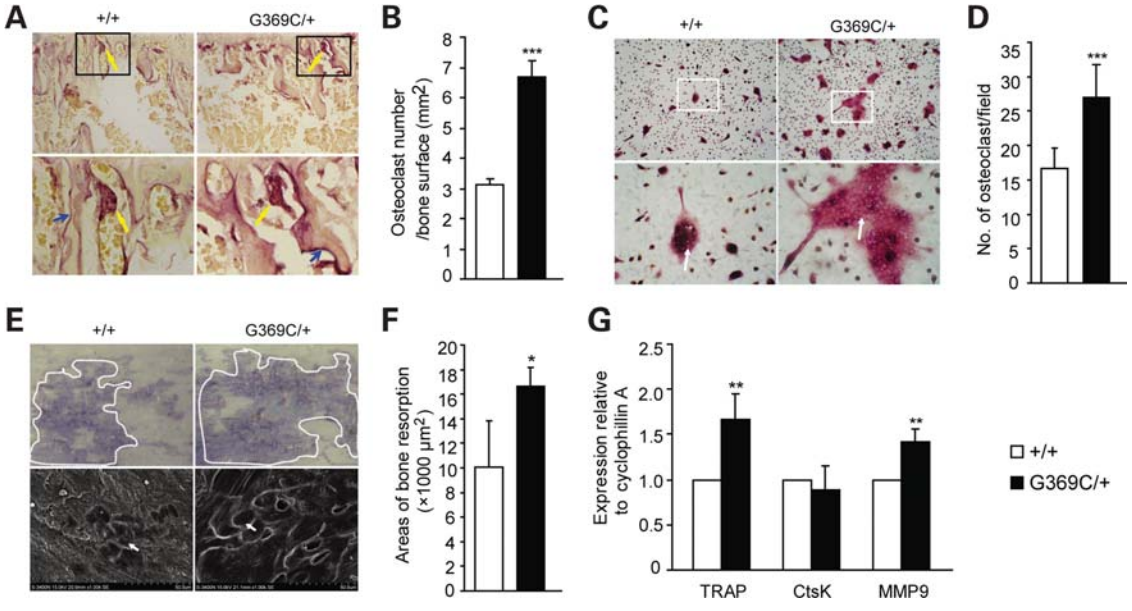

Figure 6. Enhanced osteoclast formation and bone resorption in *Fgfr3*$^{G369C/+}$ mice. (**A**) TRAP staining of tibiae from 2-month-old mice. Bottom panels show magnified views. A significantly increased number of TRAP-positive osteoclasts lining trabecular bone surfaces (top panels, yellow arrows) and larger resorpted pits (bottom panels, blue arrows) on proximal tibiae were found in *Fgfr3*$^{G369C/+}$ mice compared with wild-type mice. (**B**) Quantification of TRAP-positive cells per unit area of tibiae. *Fgfr3*$^{G369C/+}$ mice showed significantly increased number of TRAP-positive cells relative to wild-type mice ($n = 4$). (**C**) Representative images of *in vitro* osteoclast formation using cultures of non-adherent bone marrow cells for 10 days in medium containing 30 ng/ml M-CSF and 50 ng/ml RANKL. *Fgfr3*$^{G369C/+}$ mice had increased formation of large, multinuclear TRAP-positive cells compared with wild-type mice (arrows; magnification, top panels $\times 100$, bottom panels $\times 400$). (**D**) Quantification of osteoclast formation assays *in vitro* confirmed increased number of osteoclasts defined by TRAP staining in *Fgfr3*$^{G369C/+}$ mice. (**E**) Toluidine blue staining (top panels) and scanning electron microscopy observation (bottom panels) of resorption pits (bottom, arrows) on bovine cortical bone after non-adherent bone marrow cells were cultured in osteoclast differentiation medium for 15 days. These results showed that the area of pits resorpted by *Fgfr3*$^{G369C/+}$ osteoclasts was increased compared with wild-type osteoclasts (magnification, top panels $\times 60$, bottom panels $\times 1000$). (**F**) Quantification of resorption pit areas also revealed significantly increased bone resorption areas in *Fgfr3*$^{G369C/+}$ mice ($n = 4$). (**G**) Relative expressions of *TRAP*, *Ctsk* and *MMP-9* mRNA of osteoclasts cultured for 10 days, which showed enhanced expression of *TRAP* and *MMP-9* in *Fgfr3*$^{G369C/+}$ osteoclasts. Samples were evaluated in triplicate. Graphs show mean value $\pm$ SD (Student's *t*-test, $^{*}P < 0.05$, $^{**}P < 0.01$, $^{***}P < 0.001$).

by affecting the expressions of RANKL/OPG and M-CSF in osteoblasts and mesenchymal progenitor cells, the other is the direct regulation of osteoclast precursors and osteoclasts themselves (48,49).

Few studies have been reported about the role of FGFR3 in osteoclastogenesis. Valverde-Franco *et al.* (20) found *Fgfr3* null mutant mice had increased number of osteoclasts along trabecular bone. Chen *et al.* (11) found increased number of osteoclasts in the growth plate of postnatal *Fgfr3*$^{G369C/+}$ mice, although Amizuka *et al.* (50) showed that thanatophoric dysplasia type II (TD II) fetuses had enhanced osteoclastic activity in their growth plate. In this study, we found the expression of FGFR3 in osteoclasts and more osteoclasts over the trabeculae in adult *Fgfr3*$^{G369C/+}$ mice. Using *in vitro* osteoclastogenesis assay, we also found that the number of osteoclasts and bone resorption pits of *Fgfr3*$^{G369C/+}$ cultures were increased, which demonstrates that FGFR3 can directly up-regulate the differentiation and resorptive function of osteoclasts.

Since both *Fgfr3*$^{G369C/+}$ and *Fgfr3* null mice had enhanced osteoclast formation *in vivo*, these seemingly contradictory results could not be explained only by the direct regulation of osteoclastogenesis by FGFR3. We suspect that FGFR3 may also have an indirect effect on osteoclasts through its regulation of osteoblasts (48). FGF2 has been found to promote osteoclast differentiation via osteoblasts by inducing their expressions of RANKL/OPG and COX-2 (49,51). FGF18 also stimulates osteoclast formation and bone resorption in the co-culture of mouse primary osteoblasts and bone marrow cells (52). FGFR3 is expressed in osteoblasts and can be activated by FGF2 and FGF18 (1,2). Thus, FGFR3 may indirectly regulate osteoclasts via osteoblasts. Since FGFR1 is also expressed in osteoblasts and osteoclasts, it is speculated that both FGFR1 and FGFR3 may be coordinated to directly and indirectly regulate osteoclastogenesis. The indirect effect of FGFR3 on osteoclast formation and the coordination between FGFR1 and FGFR3 in osteoclastogenesis and bone resorption need to be further explored.

In summary, in this study, we characterized the bone phenotypes of adult *Fgfr3*$^{G369C/+}$ mice mimicking human ACH resulting from G375C mutation in FGFR3, and explored the mechanism for the regulation of bone remodeling by FGFR3. Our results demonstrate that activated FGFR3 results in reduced bone mass by regulating both bone formation and resorption. Moreover, we provide evidence that the Erk1/2 signaling activated by FGFR3 is mainly responsible for the decreased bone matrix mineralization of BMSCs, and the enhanced activity of p38 signaling results in the reduced replication and increased osteogenic differentiation of *Fgfr3*$^{G369C/+}$ BMSCs. Furthermore, for the first time, using *in vivo* and *in vitro* experiments, we demonstrate that FGFR3 plays a direct positive role in osteoclast formation

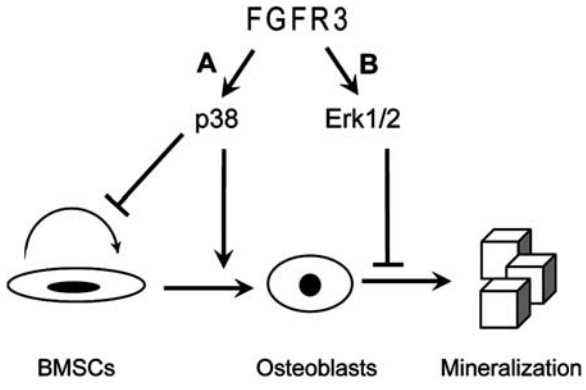

Figure 7. The effects of MAPK activated by gain-of-function mutation in FGFR3 on different stages of BMSCs. (**A**) p38 MAPK pathway inhibits BMSC proliferation, but promotes their osteogenic differentiation. (**B**) Erk1/2 MAPK pathway inhibits mineralization.

and bone resorption. All of these findings suggest that gain-of-function mutation in FGFR3 not only leads to impaired chondrogenesis, but also results in decreased bone mass in adult mice. These results deepen our understanding of the effect of FGFR3 on bone development and remodeling, as well as the pathogenesis of ACH.

MATERIALS AND METHODS

Mice

Fgfr3$^{G369C/+}$ mice were provided by Chuxia Deng of NIH (11), and all experiments were performed in accordance with protocols approved by the Institutional Animal Care and Use Committee of Daping Hospital. *Fgfr3*$^{G369C/+}$mice and littermate controls were sacrificed by exsanguination (cervical dislocation) at 2 or 4 months of age for phenotypic analyses.

Radiologic imaging and dual beam X-ray absorptiometry

The femoral bones of 2- and 4-month-old mice were harvested and stored in 70% ethanol at 4°C. High-resolution X-rays of these bones were obtained using a Faxitron MX20 (20). After X-ray detection, BMD was measured by dual energy X-ray absorptiometry (DEXA; PIXimus Mouse 11 densitometer, GE Medical System, Madison, WI, USA).

Micro-computed tomography

The femoral cancellous bones of the distal metaphysis were scanned with micro-CT (μCT-80, Scanco Medical AG, Bassersdorf, Switzerland) as previously reported (53). Image acquisition was performed at 70 kV and 113 mA. Two-dimensional images were used to generate three-dimensional reconstructions and to calculate morphometric parameters defining trabecular bone mass and micro-architecture. These include BV/TV, Tb.Th, Tb.N and Tb.Sp, as well as SMI, an indicator of plate-like versus rod-like trabecular architecture (54).

Histology and histomorphometric analysis

Two-month-old mice were weighed and injected with calcein (30 mg/kg body weight) at 10 and 3 days prior to sacrifice. The right tibiae were fixed with 40% ethanol overnight and dehydrated in a graded ethanol series. The bones were embedded in a mixture of methyl methacrylate and dibutyl phthalate for analysis of parameters of bone formation. For Von Kossa staining, five-micron-thick sections of proximal tibiae were stained with 2% silver nitrate for 20 min under UV light and with 0.1% toluidine blue for 1 min to identify mineral and osteoid, respectively. Ten-micron-thick sections were used for fluorescence observation. The BV/TV, Tb.Th, Tb.Sp and MAR of tibiae were analyzed using OsteoMeasure system (OsteoMetrics, Inc., Atlanta, GA, USA). The left tibiae were fixed in 4% paraformaldehyde overnight at 4°C, rinsed in PBS and decalcified in 15% EDTA (pH 7.4) for 20–30 days before embedding in paraffin as described previously (55). Six-micron-thick sections were used for H&E staining and staining for osteoclasts using a leukocyte acid phosphatase kit (Sigma) according to the manufacturer's instructions.

Serum biochemistry and ELISA for PINP

Serum was obtained from 2-month-old mice for total Ca and phosphate analysis using routine automated techniques at the Diagnostics Laboratory, Daping Hospital. The serum level of PTNP was detected by using IDS Mouse PINP ELA kit according to the protocol. The absorbance of stopped reaction mixtures was measured at 450 nm, color intensity developed being inversely proportional to the concentration of PINP.

BMSCs culture and inhibitor studies

BMSCs were derived from 6- to 8-week-old mice as described previously (56). Briefly, the bone marrows were flushed from the tibia and femora under aseptic conditions using α-MEM (Gibco) containing 10% FBS (Gibco). Cells were plated at a density of 5×10^5 cells/cm^2 and cultured in a humidified atmosphere of 5% CO_2 at 37°C. Medium was changed initially on day 1, then every 3 days thereafter. All assays were carried out on second passage cultures. For proliferation assay, cells were plated at 5×10^3 cells/well in 96-multiwell plates and cultured for 5 days in medium containing DMSO(Sigma), inhibitor PD98059 (20 μM) or SB203580 (20 μM) (Calbiochem). For osteogenic differentiation assay, cells were seeded at 1×10^5 cells/well in 24-multiwell plates or 5×10^5 cells/well in 6-multiwell plates. One day after plating the medium was exchanged for fresh medium supplemented with 50 μg/ml ascorbic acid, 10 mM β-glycerophosphate and 10^{-8} M dexamethasone (Sigma) containing DMSO, inhibitor PD98059 (20 μM) or SB203580 (20 μM). Medium was changed every 3 days. Osteogenic differentiation of BMSCs was assessed on day 7, 14 and 21 using ALP activity assay and staining. Mineralization was detected on day 14 and 21 by alizarin red staining.

Cell proliferation assay

Cell proliferation was detected using an *in vitro* colorimetric assay (Sigma). BMSCs were washed with PBS and incubated in 200 μl MTT solution (5 mg/ml dissolved in PBS) for 4 h at 37°C. Subsequently, MTT solution was removed and 150 μl DMSO was added. After being mixed for 10 min at room

Table 1. Primers used in this study with their sequence, length of amplification (bp), used for qRT–PCR (58–61)

Gene	Sense primer	Antisense primer	Size (bp)	Reference
Cbfal	5′-CCTGAACTCTGCACCAAGTC-3′	5′-GAGGTGGCAGTGTCATCATC-3′	234	(58)
OP	5′-TGCACCCAGATCCTATAGCC-3′	5′-TGTGGTCATGGCTTTCATTG-3′	150	(59)
OC	5′-TCTGACAAAGCCTTCATGTCC-3′	5′-AAATAGTGATACCGTAGATGCG-3′	199	(60)
Col lal	5′-AATGGTGAGACGTGGAAACCCGAG-3′	5′-CGACTCCTACATCTTCTGAGTTTGG-3′	184	(61)
TRAP	5′-GCTGGAAACCATGATCACCT-3′	5′-TTGAGCCAGGACAGCTGAGT-3′	245	
Ctsk	5′-ATTGTGACCGTGATAATGTGAA-3′	5′-GTAATGCCGCAGGCGTTGTT-3′	140	
MMP9	5′ACGGCAACGGAGAAGGCAAAC-3′	5′-TCCACTCGGGTAGGGCAGAAG-3′	162	
Cyclophillin A	5′CGAGCTCTGAGCACTGGAGA-3′	5′-TGGCGTGTAAGTCACCACC-3′	101	

temperature, the purple formazan salt product resulting from the reduction of MTT was solubilized by DMSO and quantified spectrophotometrically at 490 nm.

ALP activity and staining

ALP activity and staining was processed using ALP kit (Sigma). For ALP activity, cells were washed two times with PBS, subsequently lysed with 10 mM Tris–HCl containing 2 mM $MgCl_2$ and 0.05% Triton X-100 (pH 8.2) at 4°C. Sonicated cell lysates were then centrifuged at 12 000*g* for 10 min at 4°C, and the supernatants were used for the assays. Lysates were incubated in ALP detection buffer for 30 min at 37°C. Then the reaction was stopped by the addition of 0.1 M NaOH and monitored at 405 nm. Total protein was measured spectrophotometrically using a Micro-BCA protein assay kit (Pierce) and read at 562 nm. The enzymatic activity of ALP was normalized to the total protein content of the sample (405/562 nm). For ALP staining, cells were fixed with 4% paraformaldehyde for 10 min and stained with ALP detection solution for 30 min at 37°C, and then rinsed with PBS to remove excess staining.

Alizarin red staining of mineralized osteoblast cultures

Cell cultures were washed two times with PBS and then fixed in 70% ethanol for 1 h at 4°C. After fixation, cells were washed with water and stained with 0.2% Alizarin red (Sigma) in 2% ethanol for 15 min. Cells were then washed four times with water, and dried on 37°C. For quantification of mineral content, bound dye was dissolved with 0.5 N HCl, 5% SDS and measured at 415 nm (24).

Osteoclast formation assay

BMSCs were isolated as mentioned above. For osteoclast formation *in vitro*, the BMSCs derived from mice were plated overnight in α-MEM containing 10% FBS. Non-adherent cells were harvested, plated at 2×10^6 cells/cm^2, and cultured with 30 ng/ml M-CSF (PeproTech) and 50 ng/ml receptor activator of NF-kB ligand (RANKL; Santa Cruz), with replacement of medium every 2 days. After 10 days of culture, the cells were stained for TRAP using a leukocyte acid phosphatase kit (Sigma). TRAP-positive cells containing at least three nuclei were defined as osteoclasts, which number was counted using light microscopy. All quantifications were performed on five fields per genotype, and specimen means were calculated.

Resorption pits formation

To check the resorption activity, non-adherent bone marrow cells were plated on slices of bovine cortical bone in osteoclast differentiation medium (mentioned above) for 15 days. Then the cells on bone slices were removed with 1 M NH_4OH solution, and the resorption pits were stained with 1% toluidine blue for 1 min. The total area of pits was estimated under a light microscope with a micrometer to assess osteoclastic bone resorption using image-pro plus software (IPP 5.1). For scanning electron microscopy, bone slices were fixed in 2.5% glutaraldehyde and dehydrated in a graded ethanol series, coated with gold and viewed at 15 kV with a Hitachi S-3400N scanning electron microscope.

Real-time PCR

Total RNA of cells was isolated using Trizol reagent according to the manufacturer's instructions (Invitrogen). Primers were designed using Primer Premier 5.0 to amplify 100–250 bp sequences within the coding sequences of target genes and *Cyclophillin A* (housekeeping control). The sequences of the primers and the expected sizes of the PCR products are shown in Table 1. All reactions were performed in a Mx3000P PCR machine (Stratagene) using the Two-Step QuantiTect SYBR Green RT-PCR Kit (Takara) and reaction conditions were optimized for each of the genes by changing the annealing temperature (57°C) as described previously (55). Each run consisted of samples for genes of interest and *Cyclophillin A*. Expression levels for each gene of interest were normalized to their corresponding *Cyclophillin A* values. Each run was replicated three times.

Western blot analysis

BMSCs were micromass-cultured in the absence or presence of various reagents for the indicated time periods. Proteins were extracted with a buffer containing 50 mM Tris–HCl, pH 7.4, 150 mM NaCl, 1% Nonidet P-40, 0.1% SDS supplemented with a cooltail of protease inhibitors (Roche) (9). Protein concentrations were determined by BCA protein assay kit (Pierce). The same amounts of protein were fractionated by electrophoresis on a 10% SDS-PAGE gel, transferred to the Immobilon-P PVDF membrane (Millipore). Then the protein was probed with antibody specific to phospho-Erk1/2 and Erk1/2 (Cell Signaling) or to phospho-p38 and p38 (Cell Signaling) as described previously (57).

Statistical analysis

Data were evaluated statistically in SPSS Windows, version 10.0. Results are shown as mean ± SD. Statistics were assessed using Student's *t*-test, assuming double-sided independent variance and *P*-values were considered significant at $^{*}P < 0.05$, $^{**}P < 0.01$, $^{***}P < 0.001$ and $^{\#\#}P < 0.01$.

ACKNOWLEDGEMENT

We thank Chuxia Deng (Genetics of Development and Disease Branch, NIDDK, NIH, USA) for providing *Fgfr3*$^{G369C/+}$ mice to us, and thank Xiaofei Yun and Ning Geng (West China College of Stomatology Sichuan University, Chengdu, China) for Micro-CT analyses. And we also thank Fengtao Luo, Yaozong Zhang, Yangli Xie and Rui Zhou (Daping Hospital, Third Military Medical University, Chongqing, China) for technical support.

Conflict of Interest statement. None declared.

FUNDING

The work was supported by the Special Funds for Major State Basic Research Program of China (973 program) (No.2005CB522604), National Natural Science Foundation of China (No.30425023, No.30530410, No.30901527).

REFERENCES

1. Ornitz, D.M. and Marie, P.J. (2002) FGF signaling pathways in endochondral and intramembranous bone development and human genetic disease. *Genes Dev.*, **16**, 1446–1465.
2. Su, N., Du, X. and Chen, L. (2008) FGF signaling: its role in bone development and human skeleton diseases. *Front. Biosci.*, **13**, 2842–2865.
3. Naski, M.C. and Ornitz, D.M. (1998) FGF signaling in skeletal development. *Front. Biosci.*, **3**, d781–d794.
4. Ornitz, D.M. (2005) FGF signaling in the developing endochondral skeleton. *Cytokine Growth Factor Rev.*, **16**, 205–213.
5. Toydemir, R.M., Brassington, A.E., Bayrak-Toydemir, P., Krakowiak, P.A., Jorde, L.B., Whitby, F.G., Longo, N., Viskochil, D.H., Carey, J.C. and Bamshad, M.J. (2006) A novel mutation in FGFR3 causes camptodactyly, tall stature, and hearing loss (CATSHL) syndrome. *Am. J. Hum. Genet.*, **79**, 935–941.
6. Richette, P., Bardin, T. and Stheneur, C. (2008) Achondroplasia: from genotype to phenotype. *Joint Bone Spine*, **75**, 125–130.
7. Rousseau, F., el Ghouzzi, V., Delezoide, A.L., Legeai-Mallet, L., Le Merrer, M., Munnich, A. and Bonaventure, J. (1996) Missense FGFR3 mutations create cysteine residues in thanatophoric dwarfism type I (TD1). *Hum. Mol. Genet.*, **5**, 509–512.
8. Horton, W.A. and Lunstrum, G.P. (2002) Fibroblast growth factor receptor 3 mutations in achondroplasia and related forms of dwarfism. *Rev. Endocr. Metab. Disord.*, **3**, 381–385.
9. Rousseau, F., Bonaventure, J., Legeai-Mallet, L., Pelet, A., Rozet, J.M., Maroteaux, P., Le Merrer, M. and Munnich, A. (1994) Mutations in the gene encoding fibroblast growth factor receptor-3 in achondroplasia. *Nature*, **371**, 252–254.
10. Naski, M.C., Colvin, J.S., Coffin, J.D. and Ornitz, D.M. (1998) Repression of hedgehog signaling and BMP4 expression in growth plate cartilage by fibroblast growth factor receptor 3. *Development*, **125**, 4977–4988.
11. Chen, L., Adar, R., Yang, X., Monsonego, E.O., Li, C., Hauschka, P.V., Yayon, A. and Deng, C.X. (1999) Gly369Cys mutation in mouse FGFR3 causes achondroplasia by affecting both chondrogenesis and osteogenesis. *J. Clin. Invest.*, **104**, 1517–1525.
12. Datta, H.K., Ng, W.F., Walker, J.A., Tuck, S.P. and Varanasi, S.S. (2008) The cell biology of bone metabolism. *J. Clin. Pathol.*, **61**, 577–587.
13. Bilezikian, J.P., Matsumoto, T., Bellido, T., Khosla, S., Martin, J., Recker, R.R., Heaney, R., Seeman, E., Papapoulos, S. and Goldring, S.R. (2009) Targeting bone remodeling for the treatment of osteoporosis: summary of the proceedings of an ASBMR workshop. *J. Bone Miner. Res.*, **24**, 373–385.
14. Meyers, G.A., Orlow, S.J., Munro, I.R., Przylepa, K.A. and Jabs, E.W. (1995) Fibroblast growth factor receptor 3 (FGFR3) transmembrane mutation in Crouzon syndrome with acanthosis nigricans. *Nat. Genet.*, **11**, 462–464.
15. Arnaud-Lopez, L., Fragoso, R., Mantilla-Capacho, J. and Barros-Nunez, P. (2007) Crouzon with acanthosis nigricans. Further delineation of the syndrome. *Clin. Genet.*, **72**, 405–410.
16. Wilkes, D., Rutland, P., Pulleyn, L.J., Reardon, W., Moss, C., Ellis, J.P., Winter, R.M. and Malcolm, S. (1996) A recurrent mutation, ala391glu, in the transmembrane region of FGFR3 causes Crouzon syndrome and acanthosis nigricans. *J. Med. Genet.*, **33**, 744–748.
17. Muenke, M., Gripp, K.W., McDonald-McGinn, D.M., Gaudenz, K., Whitaker, L.A., Bartlett, S.P., Markowitz, R.I., Robin, N.H., Nwokoro, N., Mulvihill, J.J. *et al.* (1997) A unique point mutation in the fibroblast growth factor receptor 3 gene (FGFR3) defines a new craniosynostosis syndrome. *Am. J. Hum. Genet.*, **60**, 555–564.
18. Tavormina, P.L., Shiang, R., Thompson, L.M., Zhu, Y.Z., Wilkin, D.J., Lachman, R.S., Wilcox, W.R., Rimoin, D.L., Cohn, D.H. and Wasmuth, J.J. (1995) Thanatophoric dysplasia (types I and II) caused by distinct mutations in fibroblast growth factor receptor 3. *Nat. Genet.*, **9**, 321–328.
19. Karadimas, C., Trouvas, D., Haritatos, G., Makatsoris, C., Dedoulis, E., Velissariou, V., Antoniadi, T., Hatzaki, A. and Petersen, M.B. (2006) Prenatal diagnosis of achondroplasia presenting with multiple-suture synostosis: a novel association. *Prenat. Diagn.*, **26**, 258–261.
20. Valverde-Franco, G., Liu, H., Davidson, D., Chai, S., Valderrama-Carvajal, H., Goltzman, D., Ornitz, D.M. and Henderson, J.E. (2004) Defective bone mineralization and osteopenia in young adult FGFR3−/− mice. *Hum. Mol. Genet.*, **13**, 271–284.
21. Eswarakumar, V.P. and Schlessinger, J. (2007) Skeletal overgrowth is mediated by deficiency in a specific isoform of fibroblast growth factor receptor 3. *Proc. Natl. Acad. Sci. USA*, **104**, 3937–3942.
22. Franceschi, R.T. and Xiao, G. (2003) Regulation of the osteoblast-specific transcription factor, Runx2: responsiveness to multiple signal transduction pathways. *J. Cell. Biochem.*, **88**, 446–454.
23. Ge, C., Xiao, G., Jiang, D. and Franceschi, R.T. (2007) Critical role of the extracellular signal-regulated kinase-MAPK pathway in osteoblast differentiation and skeletal development. *J. Cell. Biol.*, **176**, 709–718.
24. Jacob, A.L., Smith, C., Partanen, J. and Ornitz, D.M. (2006) Fibroblast growth factor receptor 1 signaling in the osteo-chondrogenic cell lineage regulates sequential steps of osteoblast maturation. *Dev. Biol.*, **296**, 315–328.
25. Yu, K., Xu, J., Liu, Z., Sosic, D., Shao, J., Olson, E.N., Towler, D.A. and Ornitz, D.M. (2003) Conditional inactivation of FGF receptor 2 reveals an essential role for FGF signaling in the regulation of osteoblast function and bone growth. *Development*, **130**, 3063–3074.
26. Komori, T., Yagi, H., Nomura, S., Yamaguchi, A., Sasaki, K., Deguchi, K., Shimizu, Y., Bronson, R.T., Gao, Y.H., Inada, M. *et al.* (1997) Targeted disruption of Cbfa1 results in a complete lack of bone formation owing to maturational arrest of osteoblasts. *Cell*, **89**, 755–764.
27. Ducy, P., Starbuck, M., Priemel, M., Shen, J., Pinero, G., Geoffroy, V., Amling, M. and Karsenty, G. (1999) A Cbfa1-dependent genetic pathway controls bone formation beyond embryonic development. *Genes Dev.*, **13**, 1025–1036.
28. Xiao, G., Jiang, D., Thomas, P., Benson, M.D., Guan, K., Karsenty, G. and Franceschi, R.T. (2000) MAPK pathways activate and phosphorylate the osteoblast-specific transcription factor, Cbfa1. *J. Biol. Chem.*, **275**, 4453–4459.
29. Funato, N., Ohtani, K., Ohyama, K., Kuroda, T. and Nakamura, M. (2001) Common regulation of growth arrest and differentiation of osteoblasts by helix-loop-helix factors. *Mol. Cell. Biol.*, **21**, 7416–7428.
30. Zhou, Y.X., Xu, X., Chen, L., Li, C., Brodie, S.G. and Deng, C.X. (2000) A Pro250Arg substitution in mouse Fgfr1 causes increased expression of Cbfa1 and premature fusion of calvarial sutures. *Hum. Mol. Genet.*, **9**, 2001–2008.
31. Marie, P.J. (2003) Fibroblast growth factor signaling controlling osteoblast differentiation. *Gene*, **316**, 23–32.

32. Xiao, G., Jiang, D., Gopalakrishnan, R. and Franceschi, R.T. (2002) Fibroblast growth factor 2 induction of the osteocalcin gene requires MAPK activity and phosphorylation of the osteoblast transcription factor, Cbfa1/Runx2. *J. Biol. Chem.*, **277**, 36181–36187.
33. Huang, Z., Cheng, S.L. and Slatopolsky, E. (2001) Sustained activation of the extracellular signal-regulated kinase pathway is required for extracellular calcium stimulation of human osteoblast proliferation. *J. Biol. Chem.*, **276**, 21351–21358.
34. Lee, S.W., Choi, K.Y., Cho, J.Y., Jung, S.H., Song, K.B., Park, E.K., Choi, J.Y., Shin, H.I., Kim, S.Y., Woo, K.M. *et al.* (2006) TGF-beta2 stimulates cranial suture closure through activation of the Erk-MAPK pathway. *J. Cell. Biochem.*, **98**, 981–991.
35. Lai, C.F., Chaudhary, L., Fausto, A., Halstead, L.R., Ory, D.S., Avioli, L.V. and Cheng, S.L. (2001) Erk is essential for growth, differentiation, integrin expression, and cell function in human osteoblastic cells. *J. Biol. Chem.*, **276**, 14443–14450.
36. Kono, S.J., Oshima, Y., Hoshi, K., Bonewald, L.F., Oda, H., Nakamura, K., Kawaguchi, H. and Tanaka, S. (2007) Erk pathways negatively regulate matrix mineralization. *Bone*, **40**, 68–74.
37. Higuchi, C., Myoui, A., Hashimoto, N., Kuriyama, K., Yoshioka, K., Yoshikawa, H. and Itoh, K. (2002) Continuous inhibition of MAPK signaling promotes the early osteoblastic differentiation and mineralization of the extracellular matrix. *J. Bone Miner. Res.*, **17**, 1785–1794.
38. Rodriguez, J.P., Rios, S., Fernandez, M. and Santibanez, J.F. (2004) Differential activation of ERK1,2 MAP kinase signaling pathway in mesenchymal stem cell from control and osteoporotic postmenopausal women. *J. Cell Biochem.*, **92**, 745–754.
39. Kim, H.J., Lee, M.H., Park, H.S., Park, M.H., Lee, S.W., Kim, S.Y., Choi, J.Y., Shin, H.I., Kim, H.J. and Ryoo, H.M. (2003) Erk pathway and activator protein 1 play crucial roles in FGF2-stimulated premature cranial suture closure. *Dev. Dyn.*, **227**, 335–346.
40. Xiao, G., Gopalakrishnan, R., Jiang, D., Reith, E., Benson, M.D. and Franceschi, R.T. (2002) Bone morphogenetic proteins, extracellular matrix, and mitogen-activated protein kinase signaling pathways are required for osteoblast-specific gene expression and differentiation in MC3T3-E1 cells. *J. Bone Miner. Res.*, **17**, 101–110.
41. Raucci, A., Laplantine, E., Mansukhani, A. and Basilico, C. (2004) Activation of the ERK1/2 and p38 mitogen-activated protein kinase pathways mediates fibroblast growth factor-induced growth arrest of chondrocytes. *J. Biol. Chem.*, **279**, 1747–1756.
42. Suzuki, A., Guicheux, J., Palmer, G., Miura, Y., Oiso, Y., Bonjour, J.P. and Caverzasio, J. (2002) Evidence for a role of p38 MAP kinase in expression of alkaline phosphatase during osteoblastic cell differentiation. *Bone*, **30**, 91–98.
43. Hu, Y., Chan, E., Wang, S.X. and Li, B. (2003) Activation of p38 mitogen-activated protein kinase is required for osteoblast differentiation. *Endocrinology*, **144**, 2068–2074.
44. Lee, K.S., Hong, S.H. and Bae, S.C. (2002) Both the Smad and p38 MAPK pathways play a crucial role in Runx2 expression following induction by transforming growth factor-beta and bone morphogenetic protein. *Oncogene*, **21**, 7156–7163.
45. Martin, T., Gooi, J.H. and Sims, N.A. (2009) Molecular mechanisms in coupling of bone formation to resorption. *Crit. Rev. Eukaryot. Gene Expr.*, **19**, 73–88.
46. Boyle, W.J., Simonet, W.S. and Lacey, D.L. (2003) Osteoclast differentiation and activation. *Nature*, **423**, 337–342.
47. Zhao, Q., Shao, J., Chen, W. and Li, Y.P. (2007) Osteoclast differentiation and gene regulation. *Front. Biosci.*, **12**, 2519–2529.
48. Khosla, S. (2001) Minireview: the OPG/RANKL/RANK system. *Endocrinology*, **142**, 5050–5055.
49. Kawaguchi, H., Chikazu, D., Nakamura, K., Kumegawa, M. and Hakeda, Y. (2000) Direct and indirect actions of fibroblast growth factor 2 on osteoclastic bone resorption in cultures. *J. Bone Miner. Res.*, **15**, 466–473.
50. Amizuka, N.C., Chen, M.F., Goodyer, C., Sasaki, T. and Asawa, Y. (2001) Abnormalities in development of the growth plates of thanatophoric dysplasia type II fetuses result from enhanced vascular invasion and osteoclastic activity. *J. Bone Miner. Res.*, **16**, S1.
51. Chikazu, D., Hakeda, Y., Ogata, N., Nemoto, K., Itabashi, A., Takato, T., Kumegawa, M., Nakamura, K. and Kawaguchi, H. (2000) Fibroblast growth factor (FGF)-2 directly stimulates mature osteoclast function through activation of FGF receptor 1 and p42/p44 MAP kinase. *J. Biol. Chem.*, **275**, 31444–31450.
52. Shimoaka, T., Ogasawara, T., Yonamine, A., Chikazu, D., Kawano, H., Nakamura, K., Itoh, N. and Kawaguchi, H. (2002) Regulation of osteoblast, chondrocyte, and osteoclast functions by fibroblast growth factor (FGF)-18 in comparison with FGF-2 and FGF-10. *J. Biol. Chem.*, **277**, 7493–7500.
53. Montero, A., Okada, Y., Tomita, M., Ito, M., Tsurukami, H., Nakamura, T., Doetschman, T., Coffin, J.D. and Hurley, M.M. (2000) Disruption of the fibroblast growth factor-2 gene results in decreased bone mass and bone formation. *J. Clin. Invest.*, **105**, 1085–1093.
54. Hurley, M.M., Okada, Y., Xiao, L., Tanaka, Y., Ito, M., Okimoto, N., Nakamura, T., Rosen, C.J., Doetschman, T. and Coffin, J.D. (2006) Impaired bone anabolic response to parathyroid hormone in Fgf2−/− and Fgf2+/− mice. *Biochem. Biophys. Res. Commun.*, **341**, 989–994.
55. Su, N., Yang, J., Xie, Y., Du, X., Lu, X., Yin, Z., Yin, L., Qi, H., Zhao, L., Feng, J. *et al.* (2008) Gain-of-function mutation of FGFR3 results in impaired fracture healing due to inhibition of chondrocyte differentiation. *Biochem. Biophys. Res. Commun.*, **376**, 454–459.
56. Osyczka, A.M. and Leboy, P.S. (2005) Bone morphogenetic protein regulation of early osteoblast genes in human marrow stromal cells is mediated by extracellular signal-regulated kinase and phosphatidylinositol 3-kinase signaling. *Endocrinology*, **146**, 3428–3437.
57. Yin, L., Du, X., Li, C., Xu, X., Chen, Z., Su, N., Zhao, L., Qi, H., Li, F., Xue, J. *et al.* (2008) A Pro253Arg mutation in fibroblast growth factor receptor 2 (Fgfr2) causes skeleton malformation mimicking human Apert syndrome by affecting both chondrogenesis and osteogenesis. *Bone*, **42**, 631–643.
58. Kawaguchi, J., Mee, P.J. and Smith, A.G. (2005) Osteogenic and chondrogenic differentiation of embryonic stem cells in response to specific growth factors. *Bone*, **36**, 758–769.
59. Liu, Z., Shi, W., Ji, X., Sun, C., Jee, W.S., Wu, Y., Mao, Z., Nagy, T.R., Li, Q. and Cao, X. (2004) Molecules mimicking Smad1 interacting with Hox stimulate bone formation. *J. Biol. Chem.*, **279**, 11313–11319.
60. Song, C., Guo, Z., Ma, Q., Chen, Z., Liu, Z., Jia, H. and Dang, G. (2003) Simvastatin induces osteoblastic differentiation and inhibits adipocytic differentiation in mouse bone marrow stromal cells. *Biochem. Biophys. Res. Commun.*, **308**, 458–462.
61. Kato, Y., Boskey, A., Spevak, L., Dallas, M., Hori, M. and Bonewald, L.F. (2001) Establishment of an osteoid preosteocyte-like cell MLO-A5 that spontaneously mineralizes in culture. *J. Bone Miner. Res.*, **16**, 1622–1633.